ACTA NEUROBIOLOGIAE EXPERIMENTALIS

Research paper Acta Neurobiol Exp 2012, 72: 51–64

Neural generators of the auditory evoked potential components P3a and P3b

Eligiusz Wronka [1, 2]*, Jan Kaiser [1], and Anton M.L. Coenen [2]

[1]Psychophysiology Laboratory, Institute of Psychology, Jagiellonian University, Kraków, Poland,
*Email: eligiusz.wronka@gmail.com; [2]Department of Biological Psychology, Radboud University Nijmegen, Nijmegen, The Netherlands

The aim of the present study was to define the scalp topography of the two subcomponents of the P3 component of the auditory evoked potential elicited in a three-stimulus oddball paradigm and to identify their cortical generators using the standardized low resolution electromagnetic tomography (sLORETA). Subjects were presented with a random sequence of auditory stimuli and instructed to respond to an infrequently occurring target stimulus inserted into a sequence of frequent standard and rare non-target stimuli. Results show that the magnitude of the frontal P3a is determined by the relative physical difference among stimuli, as it was larger for the stimulus more deviant from the standard. Major neural generators of the P3a were localized within frontal cortex and anterior cingulate gyrus. In contrast to this, the P3b, showing maximal amplitude at parietal locations, was larger for stimuli demanding a response than for the rare non-target. Major sources of the P3b included the superior parietal lobule and the posterior part of the cingulate gyrus. Our findings are in line with the hypothesis that P3a is related to alerting activity during the initial allocation of attention, while P3b is related to activation of a posterior network when the neuronal model of perceived stimulation is compared with the attentional trace.

Key words: ERP, source localization, P3a, P3b

INTRODUCTION

The P3 component of the event-related sensory potentials (the positive wave at 300 ms latency) is consistently related to attention, decision making, and memory updating and therefore provides a valuable tool for investigation of these processes in the human brain (see Polich and Criado 2006, Polich 2007, for a review). There is also strong evidence that this component represents the summation of activity from various widely distributed areas in the brffain, and at least two subcomponents which temporally overlap can be distinguished, namely the P3a and the P3b (Polich and Criado 2006). Each of these may reflect distinct information processing events.

The P3a is a large positive deflection with a frontocentral distribution, and is typically elicited by novel or rare non-target stimuli inserted in a series of standard and target stimuli in the three-stimulus oddball paradigm. This component has relatively short peak latency (Courchesne et al. 1975, Friedman and Simpson 1994). It was previously suggested that P3a reflects an alerting process in the frontal lobe when involuntary attention has to be redirected to unexpected events (Yamaguchi and Knight 1991a). In contrast to this, the P3b (or classical P3) has a more posterior-parietal scalp distribution and a somewhat longer latency than P3a. There is broad evidence that this component can be regarded as reflecting target stimulus classification in tasks that require some form of action like a covert or overt response to stimuli (Donchin and Coles 1988, Polich 1998, Kok 2001). Specifically, the P3b has been considered as indexing voluntary attention, such that its amplitude reflects the allocation of attentional resources (Kok 2001, Wronka et al. 2007), and its peak latency is considered to be related to stimulus evaluation time (Kutas et al. 1977).

Taken together, these two components appear to differ in their scalp distribution, magnitude, and peak latency as a function of the stimulus meaning. Therefore, it can be suggested that the P3a and P3b reflect distinct

Correspondence should be addressed to E. Wronka
Email: eligiusz.wronka@gmail.com

Received 25 August 2011, accepted 27 December 2011

although strongly interrelated information processing events. Early P3a can be associated with the initial attention reallocation resulting from detection of the stimulus attribute change. This process follows original sensory processing and stimulus feature mismatch detection. Due to this, it has been previously suggested that the P3a is generally similar to the orienting response. Contrary to this, later P3b can be related to the voluntary stimulus classification. This process should engage working memory comparison, while the neuronal model of the stimulation is compared with the attentional trace of relevant information. It is reasonable to assume that the stimulus deviance detection initially engages attention (P3a) to facilitate the stimulus meaning assessment (P3b) which is associated with memory operations.

There is general agreement that both components stem from the activity of multiple neural generators. However, the exact location of these generators is still not precisely described. The frontal lobe is suggested as the source of the P3a. Patients with a frontal lesion demonstrate attenuated amplitude of the P3 recorded at frontal sites, while their parietal response can be less affected (Knight 1984, Yamaguchi and Knight 1991c, Knight et al. 1995). These data suggest that the dorsolateral prefrontal cortex makes a major contribution to the scalp recorded P3a. These results are in line with more recent neuroimaging and ERP studies demonstrating that activity of the frontal cortex can be related to detection of infrequent or alerting stimuli (Potts et al. 1996, McCarthy et al. 1997, Verbaten et al. 1997, see also Bocquillon et al. 2011 for review). A dipole analysis was also consistent with the notion of prefrontal involvement in novelty P3 generation (Mecklinger and Ullsperger 1995). This is also consistent with Baudena and coworkers (1995), where intracerebral potentials were measured in patients while they performed an auditory discrimination task with target and non-target rare stimuli. On the other hand, there is also evidence that activity within more posterior areas of the brain may play some role in the generation of the P3a component. Specifically, Halgren and others (1995b) reported potentials recorded intracerebrally from patients as the responses to auditory and visual tasks, including the three-tone oddball paradigm, as well as the passive oddball task. They suggested that activity of the temporal pole, middle temporal, parahippocampal and fusiform gyrus may be related to the non-specific orienting response that is also reflected in the scalp P3a. This is in line with reports from patients with focal hippocampal lesions, showing reduced amplitude of the P3a to novel distracters but a normal P3b component to targets (Knight 1996). Decreased P3 response was also reported for patients with lesions located in the temporal-parietal junction (Yamaguchi and Knight 1991c).

In contrast to this, there is a suggestion that neural generators of the P3b are located more posteriorly than the P3a. The more anterior located source for non-target P3 as compared to target P3 was recently reported by Barry and Rushby (2006) using LORETA source localization. This finding is consistent with results from human lesion research. Specifically, P3b amplitude is reduced after brain damage in the temporal-parietal junction (Knight et al. 1989, Yamaguchi and Knight 1991b, Verleger et al. 1994), which suggests more posterior localization of its neural source when compared to P3a. This hypothesis could also be supported by the Halgren and colleagues (1995a) findings from intracerebral recording in patients. These authors reported that activity within superior temporal gyrus and hippocampus at about 380 ms post-stimulus may be reflected in the scalp P3b. This is also in line with recent magnetoencephalographic recording and functional imaging studies demonstrating that performing an oddball task activated several brain regions including the bilateral temporal-parietal cortex, thalamus, and anterior cingulate (Menon et al. 1997, Alho et al. 1998, Li, Wang and Hu 2009, see also Bocquillon et al. 2011 for review). However, there is also evidence that dorsolateral prefrontal lesions can result in P3b reduction (Barcelo et al.2000), which suggests that frontal cortex can be involved in generation of this component.

Taken together, it is reasonable to suggest that generation of the P3a and P3b stem from widespread activation within both frontal and parieto-temporal areas. Recent neuroimaging studies show that both target detection and distracter processing can be related to increased activation of frontal as well as parietal and temporal brain areas (Ebmeier et al. 1995, Kirino et al. 2000, Kiehl et al. 2001, Bledowski et al. 2004). It should be noticed that neuroimaging techniques provide relatively poor temporal resolution. Functional magnetic resonance imaging (fMRI) can provide maps of brain activation with millimeter spatial resolution however it is limited in its temporal precision to the order of seconds. This technique enables to depict differences in brain activation elicited by distinct stimuli (e.g. targets, non-targets, standards in three-stimulus oddball task), but does not allow to define which of these differences

are specifically related to the generation of the P3a or the P3b. It is reasonable to suppose that such distinction can not be achieved in case of the hemodynamic response, which is typically delayed in onset after the neuronal activity and is prolonged in duration. For that reason, hemodynamic activity measured with fMRI in response to both targets and distracters can be rather associated with the indistinctive widespread activation underlying the whole P3 complex. Moreover, it can not be completely excluded that the brain activation pattern observed in neuroimaging studies also reflects the generation of the ERP components other than the P3 (e.g. N2). Therefore, it is difficult to say whether results obtained with fMRI and the scalp-recorded positive ERP components dubbed as the P3a and P3b actually correspond to the same physiological processes. Hence, so far it is not clear to what extent frontal and parieto-temporal brain regions are involved in generation of P3a and P3b. Topographical analysis in a normal population suggests that the response to novel events activates the neural circuit that includes the prefrontal cortex and posterior regions of the brain (Friedman et al. 1993, Fabiani and Friedman 1995). However, precise information about the role of these cortical regions in generation of the P3a and P3b is still lacking. This issue can be studied with the cortical source localization methods, which have been developed to link directly scalp-recorded ERP potentials with the cortical activition. It has recently been demonstrated that among such methods the Low Resolution Electromagnetic Tomography (LORETA) is the most promising for the source localization, especially when different cortical regions are expected to be simultaneously active (Yao and Dewald 2005). Previous LORETA studies have reported neural sources of the P3 in the prefrontal cortex, the inferior and superior parietal cortex, the temporal lobe, and the cingulum (Anderer et al. 2003, Mulert et al. 2004, Barry and Rushby 2006, Volpe et al. 2007, Wang et al. 2010, Bocquillon et al. 2011). Nevertheless, there has been, to our knowledge, no LORETA study where the activity elicited by targets and non-targets was compared separately in the P3a and P3b latency windows.

Present study

The main aim of the present study was to establish the neural generators of the P3a and P3b by recording ERPs in a three-tone oddball task and localizing the underlying activity using the Standardized Low Resolution Electromagnetic Tomography (sLORETA). The three-stimulus oddball paradigm is a modification of the oddball task in which rare non-target stimuli are inserted into a sequence of rare target and frequent standard stimuli. This procedure allows recording of clearly distinct P3a and P3b components (Wronka et al. 2008). Such distinction is not readily apparent when the traditional 2-stimulus oddball task is implemented (Polich 1988). We expect that distinguishable P3a and P3b components would be measured in response to our target and non-target auditory stimuli. However, due to the fact that participants were instructed to respond only to targets and to ignore non-targets, substantially different ERP waveforms would be elicited by each stimulus category. We predict that the early frontal P3a components measured in response to rare targets and non-targets would not differ significantly in their scalp topography. At the same time we expect the differences in their amplitudes, which can reflect different intensity of the early attention engagement, partially dependent on the physical properties of the stimulation. The greater the mismatch between the standard and rare stimuli, the stronger would be the attentional switch, and the larger would be the P3a response. Thus, we predict that non-target stimuli would elicit more evident P3a responses because the physical difference between our non-targets and standard was larger than the difference between targets and standards. Similarly, the parietal P3b responses elicited by target and non-target stimuli are not expected to differ in their scalp distribution, despite the expected differences in their amplitudes. Following many previous reports (Polich and Criado 2006, Polich 2007, for a review), we predict that P3b elicited by targets would exceed the response to non-targets. In order to determine clearly the P3 subcomponents, difference waves will be calculated by subtracting the standard stimulus ERP from ERPs elicited by targets and non-targets (Wronka et al. 2008). Neural generators of the P3a and P3b components will be separately established using the Standardized Low Resolution Electromagnetic Tomography (sLORETA). We will compare the LORETA images obtained for targets and non-targets with those computed for standard stimuli in order to determine brain regions showing differential activation during the P3a or P3b latency windows. We expect to observe activation of similar fronto-parietal network in response to targets and non-targets, which would correspond to the similarities in scalp distribution of the P3a and P3b elicited by targets

and non-targets. Moreover, we will contrast the LORETA images obtained for targets and non-targets to reveal the differences in brain activation which can be associated with the expected differences in the amplitude of the P3a and P3b components. These brain areas can be therefore directly linked with the neural processes relevant for initial attention allocation and subsequent stimulus meaning evaluation.

METHODS

Participants

Twenty eight healthy students (24 women and 4 men; mean age = 21.2; SD = 1.5 years) served as participants in the experiment. All of them were right-handed and had normal, or corrected to normal, vision, as well as normal hearing. They received course points for their participation and signed an informed consent. All participants reported being free of neurological or psychiatric disorders, and absence of drug abuse and use of medication.

Experimental procedure

The EEG session lasted about twenty minutes. Subjects were seated in a darkened sound-isolated, air-conditioned chamber. They were asked to relax and to restrict body movements and blinking as much as possible while they were presented with a random series of tones (consisting of 1000 Hz standard, 1100 Hz target, and 1200 Hz non-target tones with probabilities of 0.8, 0.1 and 0.1, respectively). They were also asked to silently count the target tones and report the total number at the end of the session. Stimulus tones were presented with random ISI (1.25–2 s) through a loudspeaker located in front of the subject at 65 dB SPL (100 ms duration with 10 ms rise/fall time).

Electrophysiological recording

The EEG was recorded using a BioSemi ActiveOne system with Ag–AgCl electrodes from 31 monopolar locations (Fp1, Fp2, F3, F4, F7, F8, FT7, FT8, FC3, FC4, T7, T8, C3, C4, TP7, TP8, CP3, CP4, P7, P8, P3, P4, O1, O2, AFz, Fz, FCz, Cz, CPz, Pz, Oz) according to the extended 10–20 system (Nuwer et al. 1998). Two additional electrodes [common mode sense (CMS) active electrode and driven right leg (DRL) passive electrode] were used as reference and ground electrodes, respectively (c.f. www.biosemi.com/faq/cms&drl.htm). All the cephalic electrodes were placed on the scalp using an Electro-Cap. The horizontal and

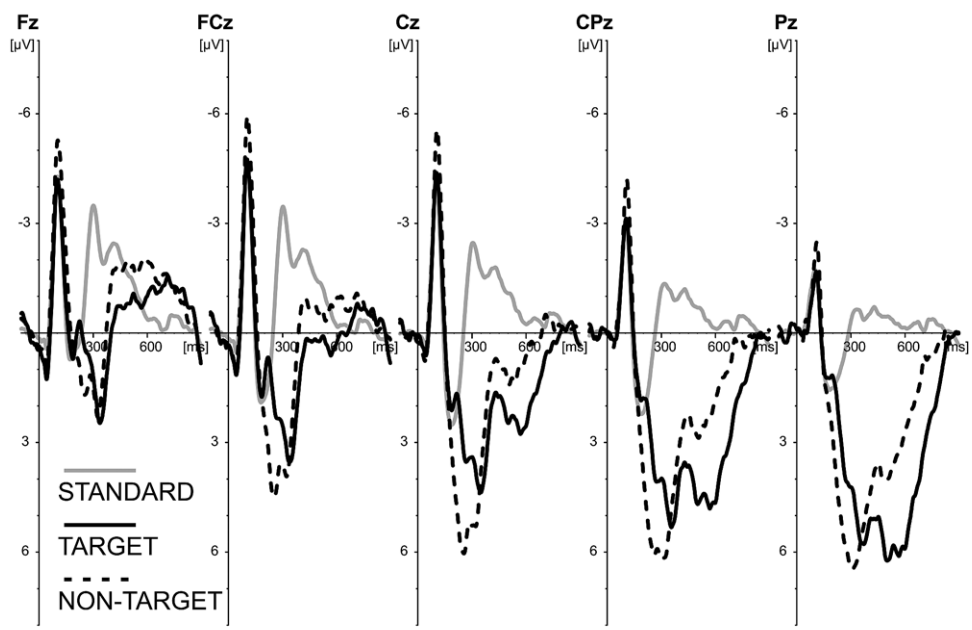

Fig. 1. Grand averaged ERP responses to standard (grey line), target (solid black line), and non-target (dashed black line) stimuli recorded at 5 midline electrodes (Fz, FCz, Cz, CPz, and Pz).

vertical EOG were monitored by an additional 4 electrodes, placed above and below the right eye and in the external canthi of both eyes. The EEG was acquired at a sampling rate of 512 Hz.

Output data were subsequently transferred to and stored in a computer for analysis. The EEG data were off-line re-referenced to an average montage, filtered with bandpass 0.016–30 Hz (24 dB), and sampled for 100 ms prior to stimulus onset and 900 ms after stimulus onset using BrainVision software. Finally, data were corrected for eye-movement artefacts (Gratton et al. 1983). The ERP components of interest were defined as the largest positive going peaks within specific latency windows: 250–400 ms, and 400–700 ms for the P3a and P3b, respectively. These windows were selected on the basis of visual inspection of grand averaged ERPs obtained for each condition. Peak amplitude was calculated relative to the pre-stimulus baseline, and peak latency was measured from the time of stimulus onset.

Repeated-measures analyses of variance (ANOVA) were performed examining the effect of within-subjects factors of electrode LOCATION (5 anterior-to-posterior locations: Fz vs. FCz vs. Cz vs. CPz vs. Pz), and STIMULUS type (target vs. non-target) on P3 mean amplitudes. These electrodes were chosen due to the fact that P3 reaches its highest amplitude at midline sites (Katayama and Polich 1998, 1999). All analyses of variance employed Greenhouse-Geisser corrections to the degrees of freedom when appropriate, and only the corrected probability values are reported. The Bonferroni method was used for *post-hoc* comparisons, with a significance level of 0.05.

Source localization – Standardized Low Resolution Electromagnetic Tomography (sLORETA)

The sources of bioelectrical activity were estimated using the 2008 version of sLORETA (free academic software available at http://www.uzh.ch/keyinst/loreta.htm). The sLORETA images reflect the three-dimensional distribution of current density. The current implementation of sLORETA used the three-shell realistic head model (Fuchs et al. 2002) and electrode coordinates provided by Jurcak (Jurcak et al. 2007). All computations were made using the template from Montreal Neurological Institute MNI (Mazziotta et al. 2001), with the three-dimensional solution space restricted to cortical gray matter and hippocampus, as determined by the probabilistic Talairach atlas (Lancaster et al. 2000). The intracerebral volume is partitioned in 6 239 voxels at 5 mm

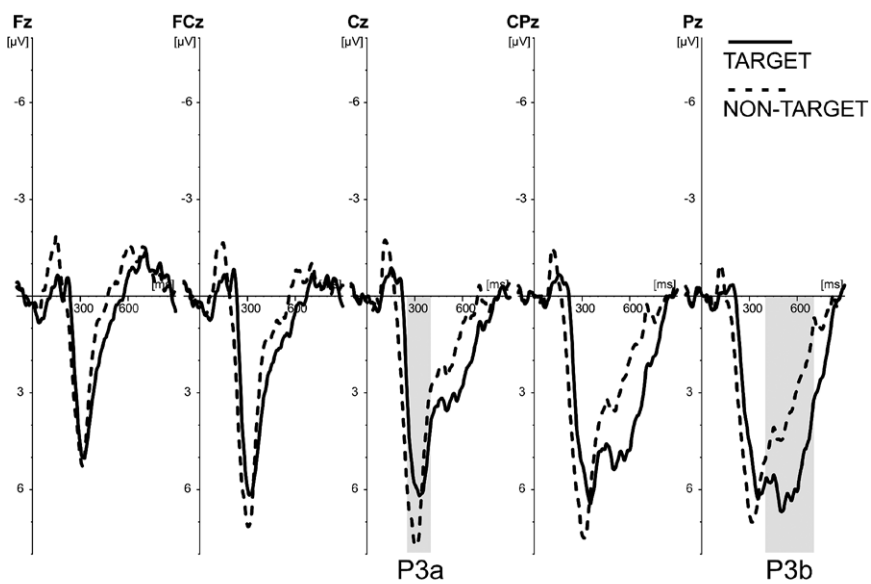

Fig. 2. Grand averaged difference waveforms computed for target minus standard difference (solid black line) and non-target minus standard difference (dashed black line) at 5 midline electrodes (Fz, FCz, Cz, CPz, and Pz).

spatial resolution. The sLORETA images represent the standardized electric activity at each voxel in neuroanatomic MNI space as the exact magnitude of the estimated current density. Anatomical labels as Brodmann areas are also reported using MNI space, with correction to Talairach space (Brett et al. 2002). The full description of the method can be found in Pascual-Marqui (2002). The proof of its exact, zero-error localization property is described by Pascual-Marqui (2007, 2009). The sLORETA images corresponding to P3a and P3b components were defined as the mean current density values for intervals between 250–400 ms post-stimuls and between 400–700 ms post-stimulus, respectively. Statistical significance of differences for sLORETA images elicited by the target and non-target stimuli was assessed with statistical nonparametric mapping tests for paired samples with correction for multiple comparisons, implemented in the version of sLORETA used (Nichols and Holmes 2002).

RESULTS

Event-related potentials

The P3a amplitude obtained in response to target stimuli was significantly smaller than the P3a evoked by non-target stimuli. Maximal amplitudes of the P3a elicited by targets and non-targets were recorded at the vertex. This result is in close agreement with previous studies suggesting a link between activity of the frontal cortex and generation of the P3a component. The amplitude of the target P3b was significantly larger than the P3b evoked by non-target stimuli. In both cases a typical topography with the maximum over parietal locations were observed. All these findings are confirmed by the statistical analyses presented in the next subsections. These effects are illustrated in Figures 1 and 2.

Amplitude of P3a

The amplitudes of the P3a component were initially assessed with a two-factor ANOVA (stimulus × location). Results obtained from the analysis suggest that a more pronounced P3a component was recorded in response to non-target stimuli when compared to targets, resulting in significant main effect of stimulus: $F_{1,27}$=7.53, P=0.011, when tested across 5 midline sites. Similarly, we found more pronounced non-target P3a response, as compared to target P3a, when analysis was restricted to vertex values: $F_{1,27}$=11.03, P=0.003. This difference is illustrated in Figures 1 and 2, which show ERP responses to target and non-target stimuli at midline electrodes. At the same time, a highly significant main effect of electrode location was also observed, $F_{4,108}$=17.71, P<0.0001, ε=0.431. This effect suggests that P3a amplitude was substantially different over the 5 midline electrodes, which was confirmed by *post-hoc* comparisons. The lowest values were obtained for the frontal Fz electrode, and a gradual increment was observed from the frontal location to the vertex, where the maximal P3a response was measured. Values obtained at parietal electrodes were lower in comparison to vertex but the difference did not reach significance. Similar topographies were observed for P3a elicited by target and non-target stimuli, which was confirmed by non-significant stimulus × location interaction, $F_{4,108}$=1.31, P=0.331, ε=0.514. This effect is illustrated in Figure 3, which shows the P3a distribution.

Amplitude of P3b

A similar two-factor ANOVA (stimulus × location) was performed for the P3b amplitude. Obtained results show that higher P3b amplitude was recorded in response to target stimuli when compared to non-targets. However, this difference did not reach the level of significance [main effect of stimulus: $F_{1,27}$=3.02, P=0.094 when tested for 5 midline electrodes]. However, when amplitudes of P3b obtained at the parietal Pz electrode was analyzed, significantly higher values were obtained for target stimuli in comparison to non-targets: $F_{1,27}$=27.44, P<0.0001. Simultaneously, a highly significant main effect of location was observed: $F_{4,108}$=67.02, P<0.0001, ε=0.411. Topography of the P3b component in response to targets and non-targets is illustrated in Figure 3. Amplitude of P3b elicited by targets and non-targets was found to be maximal at parietal locations and progressively increased from frontal to parietal regions. This effect was confirmed by *post-hoc* analysis. What should be also noticed, is the greater increase of P3b amplitude along the saggital plane for target in comparison to non-target stimuli, confirmed by a significant stimulus × location interaction: $F_{4,108}$=7.72, P=0.001, ε=0.482.

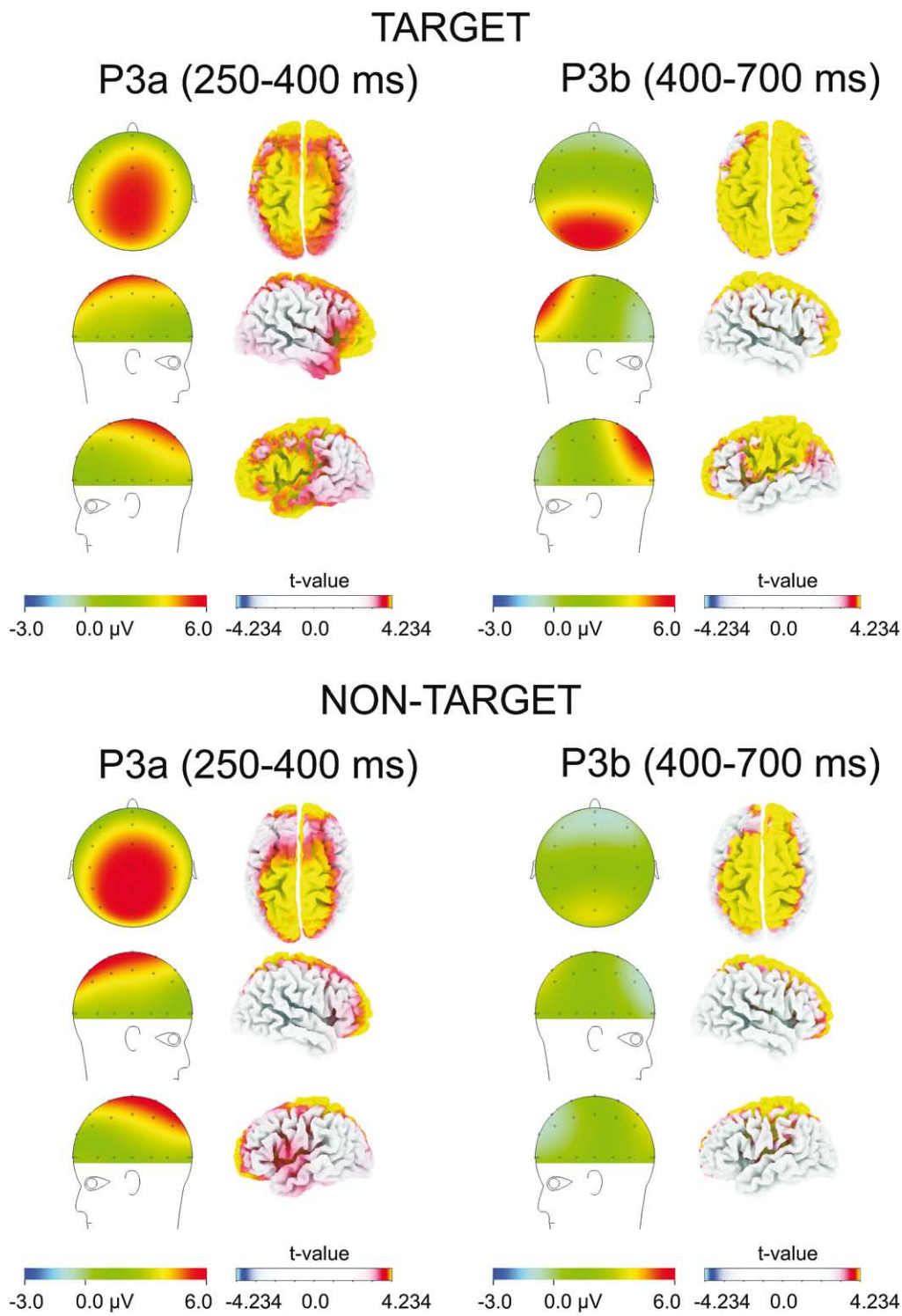

Fig. 3. ERP topographical maps showing voltage differences and corresponding sLORETA three dimensional maps of voxel-by-voxel *t*-statistics representing target minus standard difference (upper panel) and non-target minus standard difference (lower panel). The sLORETA scales show negative (blue) and positive (red) *t*-values for which the alpha is significant after Holmes' correction for multiple comparisons.

Source localization – Standardized Low Resolution Electromagnetic Tomography (sLORETA)

P3a component

The rare targets and the rare non-targets produced widespread activation within the frontal, parietal, temporal and occipital brain areas between 250 and 400 ms after stimulus onset. Significantly increased bilateral activity of several brain areas was found in response to target stimuli when compared to standards. The most pronounced differences were found within the lateral frontal lobes (inferior, middle and superior frontal gyrus) as well as for the medial part of frontal cortex (the medial frontal gyrus and anterior cingulate gyrus). These brain regions appear to be the major neural sources of P3a component. A similar effect was also observed for the insula on both sides of the brain. Slightly smaller but still significant increases of brain activity elicited by targets was also recorded within left and right parietal lobes (inferior parietal lobule, angular gyrus, supramarginal gyrus, cingulate and posterior cingulate gyri), bilaterally within the temporal areas (superior, middle, inferior temporal gyri, and fusiform gyrus), as well as within the occipital cortex (superior, middle and inferior occipital gyri, cuneus). These effects are illustrated in the top left panel of Figure 3.

We obtained a similar pattern of results when the brain response to non-targets was contrasted with activity elicited by standard stimuli for the interval between 250 and 400 ms after stimulus onset. Again, significantly higher bilateral activation within the lateral (inferior, middle, and superior frontal gyrus) as well as the medial frontal cortex (medial frontal gyrus and anterior cingulate gyrus) was observed. Higher bilateral activations of the parietal lobes (inferior parietal lobule, angular gyrus, supramarginal gyrus, cingulate and posterior cingulate gyrus), the temporal areas (superior, middle, and inferior temporal gyrus, fusiform gyrus), and the occipital cortex (superior, middle and inferior occipital gyrus, cuneus) were observed in response to non-targets when contrasted to activity elicited by standard stimuli. These findings are illustrated in the bottom left panel of Figure 3.

These results suggest that the overall pattern of activity measured within the P3a latency window is

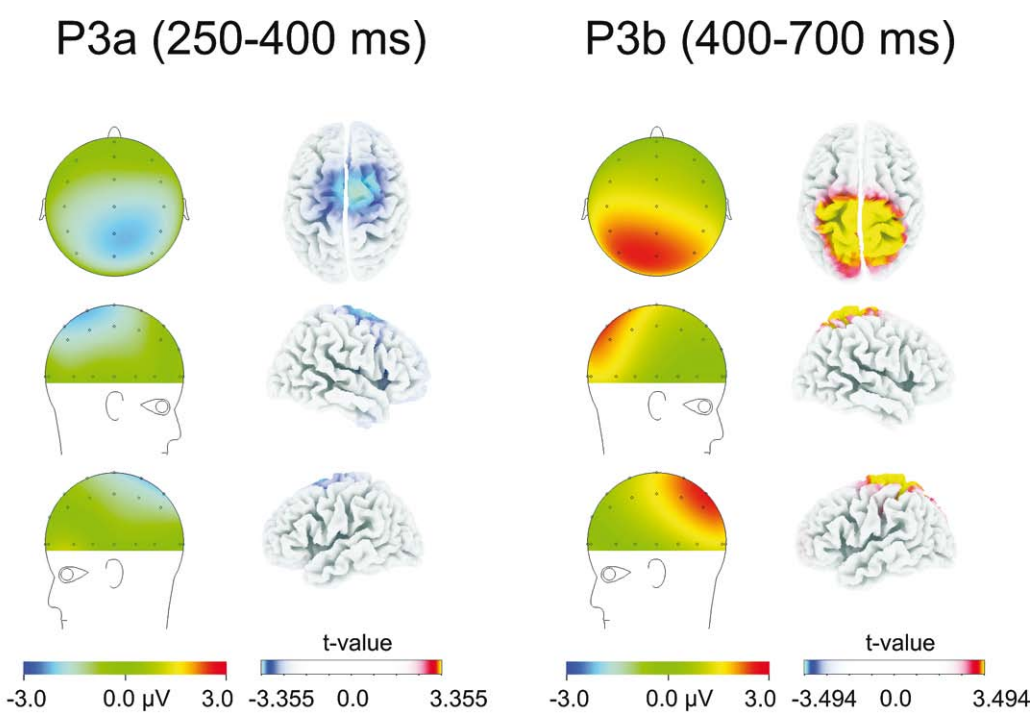

Fig. 4. ERP topographical maps showing voltage differences and corresponding sLORETA three dimensional maps of voxel-by-voxel *t*-statistics representing target minus non-target difference, corresponding to the P3a (left panel) and the P3b (right panel) latency windows. The sLORETA scales show negative (blue) and positive (red) *t*-values for which the alpha is significant after Holmes' correction for multiple comparisons.

Table I

Differences in brain activation within P3a and P3b latency windows

Comparison	Brain area	BA	MNI coordinates			*t*-score	Comparison	Brain area	BA	MNI coordinates			*t*-score
			X	*Y*	*Z*					*X*	*Y*	*Z*	
target vs. non-target P3a (250–400 ms post-stimulus)	right MeFG	6	10	0	65	-3.36	target vs. non-target P3b (400–700 ms post-stimulus)	right SPL	5	20	−45	60	4.18
	left MeFG	6	−5	−5	65	-3.27		left SPL	5	−20	−45	60	3.86
	right SFG	6	10	-5	70	−3.35		right PCL	4	5	−40	70	4.17
	left SFG	6	−5	0	70	−3.26		left PCL	4	−5	−40	60	4.15
	right CG	24	5	−5	50	−3.33		right postCG	4	10	−35	70	4.16
	left CG	24	−5	−5	50	−3.25		left postCG	4	−10	−40	60	4.10
	right MFG	6	15	5	65	−3.30		right preCG	4	35	−25	65	3.19
	left MFG	6	−15	−10	65	−3.10		left preCG	4	−35	−20	45	3.11
	right PCL	31	5	−15	50	−3.25		right SFG	6	20	−10	70	3.16
	left PCL	31	−5	−15	50	−3.19		left SFG	6	−20	−5	70	3.11
	right ACG	25	5	5	−5	−3.17		right IPL	40	30	−60	45	3.10
	left ACG	25	−5	15	−10	−3.08		left IPL	40	−35	−35	45	3.14
	right preCG	6	10	−20	70	−3.14		right PCG	31	5	−55	30	3.13
	left preCG	6	−10	−20	70	−3.03		right MeFG	6	5	−5	60	3.09
	right PHG	34	15	0	−15	−3.01		left MeFG	6	−5	−5	65	3.11
	left PHG	28	−15	−5	−15	−3.02		right preCU	31	10	−55	30	3.09
	right Reg	11	5	15	−20	−3.00		left preCU	19	−15	−85	40	3.11
	right Ins	13	30	15	15	−2.97		right CG	31	5	−60	30	3.10
	right IFG	47	15	20	−15	−2.94		left CG	31	−5	−40	30	3.11
	left IFG	47	−15	20	−15	−2.85							
	right PCG	23	5	−30	25	−2.94							
	left PCG	23	−5	−30	25	−2.92							

Brain regions showing decreased activation for target vs. non-target stimuli within the P3a latency window (250–400 ms) and increased activation for target vs. non-target stimuli within the P3b latency window (400–700 ms) at significance level ($P<0.05$).

highly similar for target and non-target stimuli. Hence, we compared sLORETA images obtained for the targets and non-targets to localize the brain regions differently activated by these stimuli. Direct comparison of the sLORETA current source density maps acquired for P3a interval revealed several brain areas where higher activation was observed bilaterally in response to non-targets compared to targets. Specifically, we found increased activity within the frontal region (inferior, middle, and superior frontal gyri, anterior cingulate and cingulate gyri, as well as medial frontal gyrus) and within temporal areas (parahippocampal gyrus and uncus). We also found significantly greater activation of the orbital gyrus and insula, but only in the right hemisphere. Other areas in which significant differences were found are summarized in Table I and illustrated in the left panel of Figure 4.

P3b component

The widespread bilateral activation of frontal, parietal, temporal and occipital brain areas were also

observed when sLORETA images obtained for the interval between 400 and 700 ms after stimulus onset in response to rare targets and rare non-targets were compared to those elicited by frequent standard stimuli. Specifically, exposition of the target stimuli leads to most evident increase of activation within the parietal lobes (superior parietal lobule, inferior parietal lobule, postcentral gyrus, posterior cingulate gyrus). This finding suggests that these brain areas are major neural sources of the P3b component. A similar bilateral effect was obtained for the lateral frontal areas (inferior, middle and superior frontal gyrus) as well as for the medial part of the frontal cortex (medial frontal gyrus and anterior cingulate gyrus). This effect was also observed for the insula on the both side of the brain.

Slightly smaller but still significant effect was also recorded bilaterally for the temporal areas (superior temporal gyrus), as well as in case of the occipital cortex (fusiform gyrus, cuneus). These effects are illustrated in the top right panel of Figure 3.

Similar pattern of results within the same latency interval (400–700 ms post-stimulus) were obtained when brain responses to non-targets were compared to activity elicited by standard stimuli. We observed significantly higher bilateral activation within the parietal (superior parietal lobule, posterior cingulate gyrus) and frontal cortex (superior frontal gyrus, middle frontal gyrus, inferior frontal gyrus, medial frontal gyrus and anterior cingulate gyrus). More pronounced activation of the temporal areas (superior temporal gyrus) was also observed in response to non-targets c.f. standard stimuli. These findings are illustrated in the bottom right panel of Figure 3.

Obtained results let us suggest that the overall pattern of activity measured within the P3b latency window is comparable for target and non-target stimuli. Therefore, we compared sLORETA images obtained for the targets and non-targets to localize the brain regions differently activated by these stimuli. Direct comparison of the sLORETA current source density maps acquired for the P3b interval revealed several brain areas where higher activation was observed bilaterally in response to targets when compared to non-targets. Specifically, we found increased activity within the parietal region (superior parietal lobule, inferior parietal lobule, paracentral lobule, postcentral gyrus, posterior cingulate gyrus) and within frontal areas (superior frontal gyrus, medial frontal gyrus). Additionally, we also found significantly greater activation of the precuneus and cuneus. Other areas, in which significant differences were found, are summarized in Table I and illustrated in the right panel of Figure 4.

DISCUSSION

The main aim of the present study was to establish the neural generators of the P3a and P3b by recording ERPs in a three-stimulus oddball task which previously has been successfully used to elicit these components separately (Wronka et al. 2008). The results of our study confirmed recent findings that the P3 complex obtained in response to rare targets and rare non-targets can be differentiated according to its amplitudes measured over frontal-central and parietal sites (Comerchero and Polich 1999, Katayama and Polich 1999). Specifically, when our experimental instruction demanded to attention resources be allocated to discrimination of auditory stimuli, evident P3 deflections were obtained for both target and non-target stimuli. In both cases, the P3 complex was divided into early P3a and late P3b components by subtracting ERPs elicited by standard tones from ERPs recorded in response to the targets or non-targets. The amplitude of the early frontal P3a was found to be larger when elicited by non-targets than targets. It is important to note that the frequency difference between the non-target stimulus and the frequent standards was twice the difference between targets and standards. This effect extends previous findings suggesting a relationship between stimulus deviance and the magnitude of the P3a response (Wronka et al. 2008). Generally, the larger is the mismatch between physical characteristics of the presented stimulus and the passively formed neuronal trace, the more intense is the initial attention engagement reflected in the P3a component (Näätänen 1990).

In contrast to this, amplitude of the P3b recorded at parietal sites to targets was larger than to non-targets. This result is consistent with many previous reports (see Polich and Criado 2006, Polich 2007, for a review), suggesting that P3b component can be related to the process of voluntary stimulus evaluation which is based on matching between the neuronal model of perceived stimulus and the previously formed attentional template of the relevant event. Our results are also in line with the suggestion that the neural generator of the P3b can be located mainly within the parietal and temporal cortices. Maximal amplitudes of this component elicited by target and non-target were obtained over parietal sites.

LORETA results obtained in our study indicated that the P3a component of the ERP can be related to increased activity within a widely distributed brain network, located predominantly within the frontal cortex. Activation of additional brain areas located within the parietal, temporal and occipital regions was also found for the P3a latency window. A highly similar pattern of effects was obtained for the target stimuli as well as for the non-targets, which is in line with the results from analysis of the ERP data, showing comparable topography of this component elicited by targets and non-targets. What is important in this context is our finding that activity within dorsolateral and medial parts of the frontal lobes can be directly linked to differences in scalp recorded P3a. Specifically, amplitude of P3a was greater in response to non-targets than targets in our study. At the same time, activity of the medial part of the frontal lobes was higher for the non-targets than targets. This finding indicates that the frontal cortex plays an important role in generating the P3a component. Therefore, it is reasonable to suggest that the activity in the dorsolateral and medial frontal areas can be directly related to initial attention reallocation following detection of stimulus change.

These findings correspond closely to previous reports from neuroimaging studies where distracter processing was linked with increased activation of both frontal and parietal brain areas (Ebmeier et al. 1995, Kirino et al. 2000, Kiehl et al. 2001, Bledowski et al. 2004). Similarly, recent source localization studies also report neural origin of the P3 in the same set of brain areas (Anderer et al. 2003, Mulert et al. 2004, Barry and Rushby 2006, Volpe et al. 2007, Wang et al. 2010, Bocquillon et al 2011). This is also consistent with the previously reported effect of P3a diminishment as the result of frontal lobe lesions (Knight 1984). Our results are also in line with data reported from studies where intracerebral potentials elicited in an auditory oddball paradigm were measured in patients (Baudena et al. 1995).

Results obtained in this study indicate also that major sources of the P3b component can be located more posterior in comparison to the P3a, which is consistent with recent LORETA studies (Barry and Rushby 2006, Volpe et al. 2007). We found that the scalp recorded P3b component can be related to enhanced activity of a broad neural network including frontal, parietal and temporal cortical regions. It should be also noted that much larger activation was observed in response to targets than to non-targets. This effect closely corresponds to differences obtained in scalp recorded EEG in our study where amplitude of the target P3b was larger than the non-target P3b. These findings are in line with previous reports where P3b to stimuli demanding overt or covert response was consistently larger than to both standard and distracter stimuli (Polich and Criado 2006). Enhanced activation of similar structures was also reported in neuroimaging studies (Ebmeier et al. 1995, Kirino et al. 2000, Kiehl et al. 2001, Bledowski et al. 2004).

Taken together, our results suggest that both P3a and P3b stem from activation of broad neuronal networks located within the frontal, parietal and temporal lobes. This network is activated when distinctive change in the environment takes place, resulting in initial attention engagement. The more salient is the stimulus, the more intense is this bottom-up process, and the more pronounced is its electrophysiological correlate – the P3a component. The larger is the mismatch, between the presentation of the actual stimulus and the neuronal trace related to previously perceived stimuli, the greater is the involuntary attention switch. In contrast to this, activity linked with P3b generation can be rather related to the later phase of information processing, when the neuronal model of the perceived stimulus is confronted with the voluntarily maintained attentional trace of the relevant event (Näätänen 1990). The more advanced this process is, the greater is the P3b amplitude.

It was recently suggested that generation of the P3a and the P3b components can be linked with the phasic activation of the neuromodulatory locus coeruleus–norepinephrine (LC-NE) system (see Nieuwenhuis et al. 2005 for details). It is important to note that the conditions when specific phasic activity of LC-NE system can be observed closely correspond to conditions under which P3 responses are measured. Specifically, LC activity in monkey have been investigated in the visual oddball task and it was found that LC neurons were phasically activated selectively by presentation of the target stimuli and only weakly or not at all by presentation of non-target stimuli. Moreover, amplitude of the LC neurons' phasic response to targets was affected by probability in a way similar to the P3. Novel stimuli typically elicit an LC phasic response and this response habituates quickly with repeated presentations. It should also be noted that there is evidence suggesting that brain

regions innervated by NE are broadly consistent with areas involved in P3 generation. Moreover, the latency differences between the frontal P3a and the more posterior P3b might be explained by the anatomy of noradrenergic fibers, which first innervate the frontal cortex and then continue caudally to more posterior cortical areas. Other neuromodulatory systems can also play an important role in P3 generation and therefore should be investigated more thoroughly. Specifically, available evidence suggests that P3a is related to frontal attention system mediated by dopaminergic activity. Parkinson disease patients who demonstrate decreased level of dopamine show also deficient P3 measures. Results from pharmacological studies have suggested that dopamine level is related to amplitude and latency of P3 (see Polich and Criado 2006 for details).

CONCLUSIONS

In conclusion, our results support the hypothesis that frontal P3a and parietal P3b components of the ERP reflect two different processes within human brain. Frontal P3a can be linked with the initial allocation of attention. The topography of this component as well as source localization data obtained in this study suggest that neural sources of P3a are located within the frontal lobe and anterior cingulate cortex. Our results also suggest that parietal P3b can be connected to the effortful evaluation of stimulus meaning. Thus, P3b is generated when the neuronal model of the stimulus is compared to the voluntarily maintained attentional trace of a relevant event. Major neural sources of the P3b were found within parietal lobe and posterior cingulate cortex. Our results are in line with the suggestion that both processes engage widespread networks of frontal and temporal-parietal cortical areas.

REFERENCES

Anderer P, Saletu B, Semlitsch HV, Pascual-Marqui RD (2003) Non-invasive localization of P300 sources in normal aging and age-associated memory impairment. Neurobiol Aging 24: 463–479.

Alho K, Winkler I, Escera C, Huotilainen M, Virtanen J, Jaaskelainen IP, Pekkonen E, Ilmoniemi RJ (1998) Processing of novel sounds and frequency changes in the human auditory cortex: Magnetoencephalographic recordings. Psychophysiology 35: 211–224.

Barcelo F, Suwazano S, Knight RT (2000) Prefrontal modulation of visual processing in humans. Nat. Neurosci. 3: 399–403.

Barry RJ, Rushby JA (2006) An orienting reflex perspective on anteriorisation of the P3 of the event-related potential. Exp Brain Res 173: 539–545.

Baudena P, Halgren E, Heit G, Clarke J (1995) Intracerebral potentials to rare target and distractor auditory and visual stimuli. III. Frontal cortex. Electroenceph Clin Neurophysiol 94: 251–264.

Bledowski C, Prvulovic D, Goebel R, Zanella FE, Linden DEJ (2004) Attentional systems in target and distractor processing: a combined ERP and fMRI study. Neuroimage 22: 530–540.

Bocquillon P, Bourriez J-L, Palmero-Soler E, Betrouni N, Houdayer E, Derambure P, Dujardin K (2011) Use of swLORETA to localize the cortical sources of target- and distracter-elicited P300 components. Clin Nerophysiol 122: 1991–2002.

Brett M, Johnsrude IS, Owen AM (2002) The problem of functional localization in the human brain. Nat Rev Neurosci 3: 243–249.

Comerchero MD, Polich J (1999) P3a and P3b from typical auditory and visual stimuli. Clin Neurophysiol 110: 24–30.

Courchesne E, Hillyard SA, Galambos R (1975) Stimulus novelty, task relevance and the visual evoked potential in man. Electroenceph Clin Neurophysiol 39: 131–143.

Donchin E, Coles MGH (1988) Is the P300 component a manifestation of context updating. Behav Brain Sci 11: 357–374.

Ebmeier KP, Steele JD, MacKenzie DM, O'Carroll RE, Kydd RR, Glabus MF, Blackwood DHR, Rugg MD, Goodwin GM (1995) Cognitive brain potentials and regional cerebral blood flow equivalents during two- and three-sound auditory ''oddball tasks''. Electroencephalogr Clin Neurophysiol 95: 434–443.

Fabiani M, Friedman D (1995) Changes in brain activity patterns in aging: the novelty oddball. Psychophysiology 32: 579–594.

Friedman D, Simpson G, Hamberger M (1993) Age-related changes in scalp topography to novel and target stimuli. Psychophysiology 30: 383–396.

Friedman D, Simpson GV (1994) ERP amplitude and scalp distribution to target and novel events: Effects of temporal order in young, middle-aged and older adults. Cogn Brain Res 2: 49–63.

Fuchs M, Kastner J, Wagner M, Hawes S, Ebersole JS (2002) A standardized boundary element method volume conductor model. Clin Neurophysiol 113: 702–712.

Gratton G, Coles MGH, Donchin E (1983) A new method for off-line removal of ocular artifact. Electroenceph Clin Neurophysiol 55: 468–484.

Halgren E, Baudena P, Clarke J, Heit G, Liegeois C, Chauvel P, Musolino A (1995a) Intracerebral potentials to rare target and distractor auditory and visual stimuli. I. Superior temporal plane and parietal lobe. Electroenceph Clin Neurophysiol 94: 191–220.

Halgren E, Baudena P, Clarke J, Heit G, Marinkovic K, Devaux B, Vignal, J-P, Biraben A (1995b) Intracerebral potentials to rare target and distractor auditory and visual stimuli. II. Medial, lateral and posterior temporal lobe. Electroenceph Clin Neurophysiol 94: 229–250.

Jurcak V, Tsuzuki D, Dan I (2007) 10/20, 10/10, and 10/5 systems revisited: Their validity as relative head-surface-based positioning systems. NeuroImage 34: 1600–1611.

Katayama J., Polich J (1998) Stimulus context determines P3a and P3b. Psychophysiology 35: 23–33.

Katayama J, Polich J (1999) Auditory and visual P300 topography from a 3 stimulus paradigm. Clin Neurophysiol 110: 463–468.

Kiehl KA, Laurens KR, Duty TL, Forster BB, Liddle PF (2001) Neural sources involved in auditory target detection and novelty processing: an event-related fMRI study. Psychophysiology 38: 133–142.

Kirino E, Belger A, Goldman-Rakic P, McCarthy G (2000) Prefrontal activation evoked by infrequent target and novel stimuli in a visual target detection task: an event-related functional magnetic resonance imaging study. J Neurosci 20: 6612–6618.

Kok A (2001) On the utility of P3 amplitude as a measure of processing capacity. Psychophysiology 38: 557–577.

Knight RT (1984) Decreased response to novel stimuli after prefrontal lesions in man. Electroenceph Clin Neurophysiol 59: 9–20.

Knight RT (1996) Contribution of human hippocampal region to novelty detection. Nature 383: 256–259.

Knight RT, Scabini D, Woods D, Clayworth C (1989) Contributions of temporal parietal junction to the human auditory P3. Brain Res 502: 109–116.

Knight RT, Grabowecky M, Scabini D (1995) Role of human prefrontal cortex in attention control. Adv Neurol 66: 21–34.

Kutas M, McCarthy G, Donchin E (1977) Augmenting mental chronometry: The P300 as a measure of stimulus evaluation time. Science 197: 792–795.

Lancaster JL, Woldorff MG, Parsons LM, Liotti M, Freitas CS, Rainey L, Kochunov PV, Nickerson D, Mikiten SA, Fox PT (2000) Automated Talairach Atlas labels for functional brain mapping. Hum Brain Mapp 10: 120–131.

Li Y, Wang LQ, Hu Y (2009) Localizing P300 generators in high-density event- related potential with fMRI. Med Sci Monit 15: MT47–53.

Mazziotta J, Toga A, Evans A, Fox P, Lancaster J, Zilles K, Woods R, Paus T, Simpson G, Pike B, Holmes C, Collins L, Thompson P, MacDonald D, Iacoboni M, Schormann T, Amunts K, Palomero-Gallagher N, Geyer S, Parsons L, Narr K, Kabani N, Le Goualher G, Boomsma D, Cannon T, Kawashima R, Mazoyer B (2001) A probabilistic atlas and reference system for the human brain: International Consortium for Brain Mapping (ICBM). Philos Trans R Soc Lond B Biol Sci 356: 1293–1322.

McCarthy G, Luby M, Gore J, Goldman-Rakic P (1997) Infrequent events transiently activate human prefrontal and parietal cortex as measured by functional MRI. J Neurophysiol 77: 1630–1634.

Mecklinger A, Ullsperger P (1995) What makes a category a category? ERP correlates of stimulus-to-category assignments. Electroencephalogr Clin Neurophysiol Suppl 44: 255–260.

Menon V, Ford JM, Lim KO, Glover GH, Pfefferbaum A (1997) Combined event-related fMRI and EEG evidence for temporal–parietal cortex activation during target detection. Neuroreport 8: 3029–3037.

Mulert C, Pogarell O, Juckel G, Rujescu D, Giegling I, Rupp D, Mavrogiorgou P, Bussfeld P, Gallinat J, Möller HJ, Hegerl U (2004) The neural basis of the P300 potential. Focus on the time-course of the underlying cortical generators. Eur Arch Psychiatry Clin Neurosci 254: 190–198.

Näätänen R (1990) The role of attention in auditory information processing as revealed by event-related potentials and other brain measures of cognitive function. Behav Brain Sci 13: 201–287.

Nieuwenhuis S, Aston-Jones G, Cohen JD (2005) Decision making, the P3, and the Locus Coerulesus-Norepinephrine system. Psychol Bull 131: 510–532.

Nichols TE, Holmes AP (2002) Nonparametric permutation tests for functional neuroimaging: a primer with examples. Hum Brain Mapp 15: 1–25.

Nuwer MC, Comi G, Emerson R, Fugslang-Frederiksen A, Guerit J-M, Hinrichs H, Ikeda A, Luccas FJC, Rappelsburger P (1998) IFCN standards for digital recording of clinical EEG. Electroenceph Clin Neurophysiol 106: 259–261.

Pascual-Marqui RD (2002) Standardized low-resolution brain electromagnetic tomography (sLORETA): technical details. Method Find Exp Clin Pharmacol 24: 5–12.

Pascual-Marqui RD (2007) Discrete, 3D distributed, linear imaging methods of electric neuronal activity. Part 1: exact, zero error localization. arXiv:0710.3341 [math-ph], http://arxiv.org/abs/0710.3341

Pascual-Marqui RD (2009) Theory of the EEG inverse problem. In: Quantitative EEG Analysis Methods and Clinical Applications (Tong S, Thankor NV, Eds). Artech House, Boston, MA, p. 121–140.

Polich J (1988) Bifurcated P300 peaks: P3a and P3b revisited? J Clin Neurophysiol 5: 287–294.

Polich J (1998) P300 clinical utility and control of variability. J Clin Neurophysiol 15: 14–33.

Polich J (2007) Updating P300: an integrative theory of P3a and P3b. Clin Neurophysiol 118: 2128–2148.

Polich J, Criado JR (2006) Neuropsychology and neuropharmacology of P3a and P3b. Int J Psychophysiol 60: 172–185.

Potts G, Liotti M, Tucker D, Posner MI (1996) Frontal and inferior temporal cortical activity in visual target detection: evidence from high spatially sampled event-related potentials. Brain Topogr 9: 3–14.

Verbaten M, Huyben M, Kemner C (1997) Processing capacity and the frontal P3. Int J Psychophysiol 25: 237–248.

Verleger R, Heide W, Butt C, Kompf D (1994) Reduction of P3b in patients with temporo–parietal lesions. Cogn Brain Res 2: 103–116.

Volpe U, Mucci A, Bucci P, Merlotti E, Galderisi S, Maj M (2007) The cortical generators of P3a and P3b: A LORETA study. Brain Res Bull 73: 220–230.

Wang J, Tang Y, Li C, Mecklinger A, Xiao Z, Zhang M, Hirayasu Y, Hokama H, Li H (2010) Decreased P300 current source density in drug-naive first episode schizophrenics revealed by high density recording. Int J Psychophysiol 75: 249–257.

Wronka E, Kuniecki M, Kaiser J, Coenen AML (2007) The P3 produced by auditory stimuli presented in a passive and active condition: modulation by visual stimuli. Acta Neurobiol Exp (Wars) 67: 155–164.

Wronka E, Kaiser J, Coenen AML (2008) The auditory P3 from passive and active three-stimulus oddball paradigm Acta Neurobiol Exp (Wars) 68: 362–372.

Yamaguchi S, Knight RT (1991a) P300 generation by novel somatosensory stimuli. Electroenceph Clin Neurophysiol 78: 50–55.

Yamaguchi S, Knight RT (1991b) Age effects on the P300 to novel somatosensory stimuli. Electroenceph Clin Neurophysiol 78: 297–301.

Yamaguchi S, Knight RT (1991c) Anterior and posterior association cortex contributions to the somatosensory P300. J Neurosci 11: 2039–2054.

Yao J, Dewald JPA (2005) Evaluation of different cortical source localization methods using simulated and experimental EEG data. Neuroimage 25: 369–382.